TRENDS IN SCIENCES 2026; 23(7): 12852
https://doi.org/10.48048/tis.2026.12852 RESEARCH ARTICLE

Sustainable EMI Shielding Composites from Recycled PE/PP and Coconut Shell–Derived Activated Carbon

Waroonsiri Jakrabutr[1], Kullawadee Sungsanit[1], Suchalinee Mathurosemontri[1], Nichanan Phansroy[1], Phongsuk Ampha[2], Nathapong Sukhawipat[3,4], Jureeporn Yuennan[5] and Wichain Chailad[1,*]

[1]Department of Materials and Metallurgical Engineering, Faculty of Engineering, Rajamangala University of Technology Thanyaburi, Pathum Thani 12110, Thailand
[2]Department of Electronics and Telecommunication Engineering, Faculty of Engineering, Rajamangala University of Technology Thanyaburi, Pathum Thani 12110, Thailand
[3]Department of Mechanical Engineering Technology, College of Industrial Technology, King Mongkut's University of Technology North Bangkok, Bangkok 10800, Thailand
[4]Center of Sustainable Energy and Engineering Materials, College of Industrial Technology, King Mongkut's University of Technology North Bangkok, Bangkok 10800, Thailand
[5]Surface Technology Research Unit (STRU), Nakhon Si Thammarat Rajabhat University, Nakhon Si Thammarat 80280, Thailand

([*]Corresponding author's e-mail: wichain_c@rmutt.ac.th)

Received: 30 November 2025, Revised: 23 December 2025, Accepted: 30 December 2025, Published: 10 March 2026

Abstract

This work explores the use of coconut-shell-derived activated carbon (AC) to improve the properties of recycled polyethylene/polypropylene (PE/PP) composites. AC was added at 0 - 25 wt% using melt blending followed by compression moulding. As the AC content increased, the composite density rose from 0.8987 to 0.9627 g/cm³, while the melt flow index dropped from 58.29 to 17.47 g/10 min, reflecting reduced chain mobility and stronger interactions between the filler and polymer matrix. Mechanical properties also improved, with the tensile modulus and tensile strength reaching 1643 and 16.8 MPa, together with a noticeable increase in ductility. DSC analysis showed two melting transitions at around 128 and 163 °C, and both the crystallization temperature (122.24 °C) and crystallization enthalpy (574 J/g at 5 wt% AC) increased, confirming that AC acts as an effective nucleating agent. The EMI-shielding performance of the composites improved steadily with AC loading. The best attenuation was obtained at 25 wt% AC, where the transmitted signal reached –18.64 dBμV at 3.82 GHz. This enhancement is attributed to the development of semi-continuous conductive pathways and stronger dielectric loss mechanisms. Overall, the results show that incorporating bio-based AC into recycled PE/PP is a practical and sustainable way to produce lightweight, low-cost composites with improved mechanical performance and effective EMI-shielding capability for use in electronic and packaging applications.

Keywords: Polyethylene, Polypropylene, Recycled PE/PP, Activated carbon, EMI shielding, Mechanical properties, Thermal behavior

Introduction

The rapid production of electronic devices and wireless communication systems has led to increasing concerns about electromagnetic interference (EMI) in everyday life. Uncontrolled EMI can disrupt the performance of sensitive equipment and cause health risks, so effective shielding materials are necessary [1,2]. Traditionally, enclosures or coatings made of metals (e.g., copper or aluminum) have been used for

EMI shielding due to their high electrical conductivity [3,4]. However, metal-based shields suffer from inherent drawbacks such as high density, susceptibility to corrosion, and poor flexibility, which limit their practicality for many modern applications [5-7]. Moreover, metallic shields primarily reflect electromagnetic waves, potentially causing secondary interference, and they tend to be expensive to process into lightweight, complex forms [4,6]. These limitations have driven the search for alternative EMI shielding materials that are lighter, more corrosion-resistant, and cost-effective.

Polymer-based composites have emerged as promising alternatives to traditional metals for EMI shielding materials [8-10]. Polymers offer advantages of low weight, chemical resistance, and ease of production, but they are fundamentally insulating and require conductive or magnetic fillers to attenuate electromagnetic waves [11]. By incorporating conductive fillers into a polymer matrix, lightweight conductive polymer composites (CPCs) can be created that dissipate or absorb EMI through a combination of reflection and absorption mechanisms [12,13]. Carbon-based fillers have been extensively explored in such composites because of their excellent electrical properties and relatively low density. For example, carbon black (CB), graphite, carbon fibers, carbon nanotubes, and graphene have all been used to impart conductivity and EMI shielding effectiveness in polymers [11,13]. These carbon-filled composites can achieve high shielding performance while retaining the processing flexibility of plastics. However, many high-performance fillers (e.g., carbon nanotubes or graphene nanoplatelets) are costly or require sophisticated production, which can offset the economic and environmental benefits of using polymers [14,15].

In recent years, increasing attention has been paid to how filler-induced microstructural networks influence the functional performance of polymer-based electromagnetic interference (EMI) shielding composites. In these materials, the development of conductive or semi-continuous filler networks within an otherwise insulating polymer matrix plays a key role in controlling electrical conductivity, dielectric loss, and overall shielding effectiveness [16,17]. Carbon-based fillers are particularly attractive in this context, as their interconnected networks promote charge transport, interfacial polarization, and multiple internal reflections of electromagnetic waves, leading to shielding behavior that is dominated by absorption rather than simple surface reflection. The efficiency of such networks is strongly affected by filler loading, dispersion quality, and the degree of interfacial contact between the filler and the polymer phases [18,19]. Therefore, establishing clear linksbetween microstructural network formation and structure-property-function relationships is essential for the rational design of lightweight, cost-effective, and sustainable EMI shielding materials.

Alongside these fundamental advances in EMI shielding mechanisms, increasing emphasis has been placed on developing sustainable EMI shielding materials using resources derived from waste [20,21]. One approach is to replace virgin or high-cost fillers with carbonaceous materials obtained from abundant waste streams. Activated carbon (AC) derived from biomass waste has garnered attention as a low-cost, sustainable filler for EMI shielding composites [22,23]. AC, such as those produced from coconut shell, are characterized by a high carbon content, extensive porous structure, and decent electrical conductivity, which enable them to absorb and attenuate electromagnetic radiation efficiently through dielectric loss and multiple internal reflections in their pores [24,25]. Furthermore, AC fillers from agricultural by-products are inexpensive and renewable compared to synthetic nanocarbons. Studies have demonstrated that polymer composites filled with AC can exhibit useful antistatic and EMI shielding properties, highlighting AC as a sustainable functional filler. Using waste-derived AC provides an effective way to recycle agro-waste (e.g., coconut shell, wood sawdust, or even animal waste-derived carbon) into value-added products, aligning with the principles of circular economy and environmental sustainability [23,26].

Complementing the use of recycled fillers, the polymer matrix itself can be sourced from post-consumer plastic waste to create fully sustainable composites. Polyolefins like polyethylene (PE) and polypropylene (PP) constitute a large fraction of global plastic waste and are attractive candidates for recycling into new materials [27,28]. In particular, low-density polyethylene (LDPE) and polypropylene (PP) are often found together in mixed plastic waste streams (e.g., packaging materials) and reusing them in combination

avoids the need for energy-intensive separation [29]. Blending LDPE and PP can also leverage the complementary properties of each polymer to achieve a balanced performance. LDPE is generally flexible and impact-resistant with a low melting point, whereas PP provides higher stiffness, strength, and thermal stability [30,31]. When combined as a blend, recycled PE/PP matrices can potentially maintain good toughness and processability while improving the dimensional stability at elevated temperatures of composites [32]. Such PE/PP blends have shown the ability to balance mechanical and thermal properties, which is advantageous for EMI shielding applications that demand both structural integrity and heat resistance in service. Notably, both the polymer blend matrix and the AC filler in this work are obtained from post-consumer and agricultural waste sources, emphasizing the sustainable nature of the material design.

Despite the evident benefits, fully waste-derived EMI shielding composites remain relatively unexplored. Prior studies on EMI shielding often use virgin polymers or expensive conductive additives, and only a limited number have incorporated recycled polymers or waste-based fillers [33]. The development of composites where both the matrix and the filler originate from recycled waste addresses a critical gap in the pursuit of green electronic materials. Therefore, this research aims to develop and characterize EMI shielding composites made entirely from waste-derived constituents: A recycled PE/PP blend reinforced with coconut shell-derived activated carbon. The introduction of porous AC into the polyolefin blend is expected to provide effective electromagnetic attenuation through absorption-dominated shielding. At the same time, the PE/PP matrix offers a balanced set of mechanical and thermal properties. In this work, the structure-property relationships of these sustainable composites were investigated, examining how factors such as filler loading and microstructure influence the electromagnetic shielding effectiveness as well as the mechanical performance. The outcomes demonstrate a feasible route to convert plastic, and biomass wastes into value-added EMI shielding materials, contributing both to waste reduction and to the development of lightweight, affordable shielding solutions for electronic applications.

Materials and methods

Materials

Recycled polyethylene (PE) and polypropylene (PP) were used as the polymer matrix. Both were sourced from post-consumer packaging waste and pelletized prior to processing. A 1:1 weight ratio of PE to PP was selected to balance flexibility and thermal resistance. Activated carbon (AC), as shown in **Figure 1**, was obtained from Carbokarn Co., Ltd. (Bangkok, Thailand) and used as received. It was derived from coconut shell and had a nominal particle size of around 74 μm (mesh 200), as specified by the supplier, with an iodine number of 950 mg/g, corresponding to its iodine adsorption capacity, which is commonly used as an indicator of high microporous surface area in activated carbon materials. No compatibilizers or surface treatments were applied. The SEM micrograph in **Figure 1** reveals the irregular morphology of the AC particles, characterized by a rough, porous surface and the presence of fine micro- and mesopores. These textural features provide abundant adsorption sites and are expected to enhance filler-matrix interaction through mechanical interlocking.

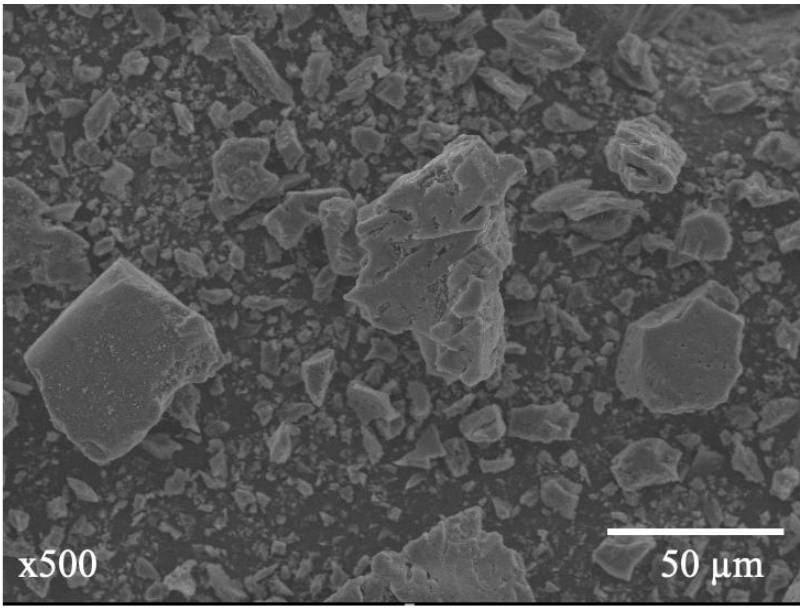

Figure 1 SEM image of AC.

Composite preparation

The recycled PE and PP pellets were dry mixed with AC powder at filler loadings of 0, 5, 10, 15, 20 and 25 wt%. Mixing was carried out using a two-roll mill at 180 °C to ensure homogeneous dispersion of the filler. The blended materials were then compression molded into flat sheets of 2 - 3 mm thickness at 180 °C under 10 MPa for 5 min, followed by cooling under pressure to room temperature. Specimens for mechanical and thermal testing were CNC-machined from molded composite sheets. The corresponding formulation compositions, expressed in grams based on a total batch mass of 100 g, are presented in **Table 1**.

Table 1 Formulations of the recycled PE/PP blend and activated carbon (total batch mass = 100 g).

Samples	PE/PP blend recycle (g)	Activated carbon (g)
Recycled PE/PP (unfilled)	100	0
Recycled PE/PP + 5 wt% AC	95	5
Recycled PE/PP + 10 wt% AC	90	10
Recycled PE/PP + 15 wt% AC	85	15
Recycled PE/PP + 20 wt% AC	80	20
Recycled PE/PP + 25 wt% AC	75	25

Mechanical properties

Tensile testing

Tensile strength and elongation at break were measured according to **ASTM D638** using a universal testing machine. Dog-bone specimens were CNC-machined from composite sheets. Testing was performed at room temperature, and the results were reported as mean values from at least five replicates.

Impact testing

Impact strength was evaluated using the **Izod method (ASTM D256)**. Notched specimens were prepared with dimensions of **12.7 mm (width)×63.5 mm (length)×3.0 mm (thickness)**. Impact tests were performed with a **2 J pendulum**. The absorbed energy was recorded and converted to impact strength (kJ/m²), averaged over three replicates per formulation.

Density

Density was determined following ASTM D792 using the immersion method. Each specimen was weighed in air and then in distilled water using an electronic balance with a density determination kit. The results were calculated based on Archimedes' principle and reported as the average of three measurements**.**

Melt Flow Index (MFI)

MFI was measured in accordance with ASTM D1238. Approximately 8 g of each sample was loaded into the barrel and tested at 190 °C under a load of 2.16 kg. The MFI was recorded in g/10 min, and three replicates were tested per condition.

Thermal analysis

Differential Scanning Calorimetry (DSC) was performed following ASTM D3418. About 1 mg of each sample was sealed in an aluminum pan and tested under a nitrogen atmosphere. The temperature program ranged from 25 - 200 °C at a heating and cooling rate of 10 °C/min. The melting temperature (T_m) and crystallization temperature (T_c) were recorded, and enthalpy values were used to assess crystallinity.

Electromagnetic interference (EMI) shielding

EMI shielding effectiveness was tested using a Diamond Engineering (DE) System in an anechoic chamber. Composite sheets (approx. 40×40 cm^2, 3 mm thickness) were mounted vertically using flexible clamp arms on a rotating platform. Measurements were performed over the frequency range of 1 - 6 GHz using horn and biconical antennas paired with a spectrum analyzer.

Each formulation was tested under two conditions, first without a copper backing (to assess absorption), and with a copper backing (to enhance internal wave reflection and total attenuation). The reflection coefficient (S11) and absorption performance were recorded. Each formulation was tested in four replicates.

Morphological analysis

Morphology of the fractured surfaces was examined using Scanning Electron Microscopy (SEM) to investigate filler dispersion and interfacial adhesion between the AC and polymer matrix. Samples were cryogenically fractured in liquid nitrogen to preserve structural features. Prior to imaging, the specimens were sputter-coated with a thin layer of gold to prevent charging and improve surface conductivity. SEM observations were performed under an accelerating voltage of 10 - 15 kV, and representative micrographs were captured for each formulation.

Results and discussion

Morphological analysis (SEM)

The fractured surfaces of recycled PE/PP-AC composites were examined by scanning electron microscopy (SEM) to evaluate the dispersion of AC and its interfacial adhesion with the recycled polymer matrix, as presented in **Figure 2**. The unfilled recycled PE/PP blend exhibits a relatively smooth and homogeneous fracture surface, typical of thermoplastic blends with good phase compatibility, which also was found by the study of Nassar *et al.* [34]. After incorporating 5 wt% AC, the surface becomes noticeably rougher with small, well-dispersed particles embedded within the matrix. This microstructure suggests effective filler wetting and mechanical interlocking between the recycled polymer chains and AC particles.

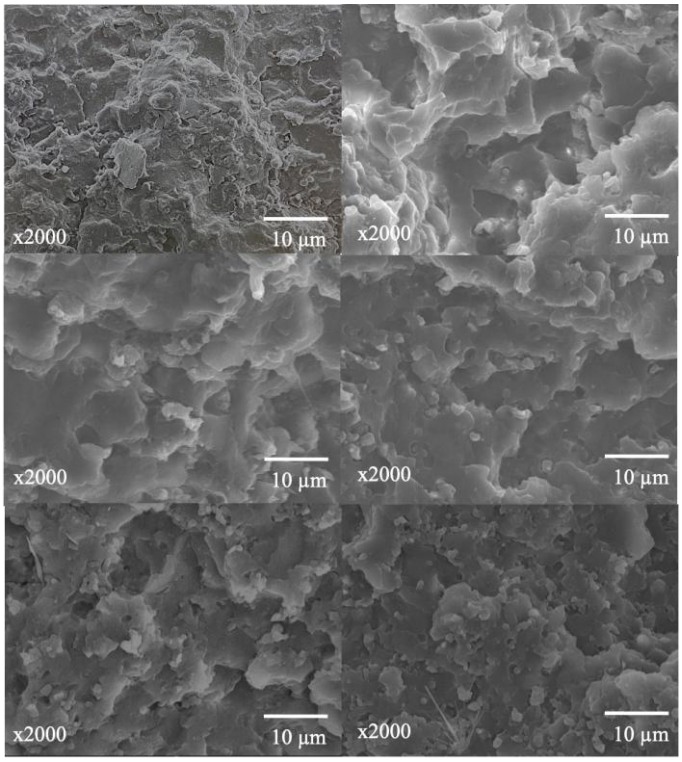

Figure 2 SEM micrographs of fractured surfaces of recycled PE/PP-AC composites at various AC loadings.

At 10 - 15 wt% AC, a more complex and finely textured morphology is observed. The fractured surfaces show numerous micro voids and fibrillation traces, indicating restricted polymer chain movement caused by AC reinforcement. These features demonstrate that moderate AC addition improves the interfacial adhesion and stress-transfer capability of the recycled PE/PP matrix. When the filler content increases to 20 - 25 wt%, the SEM micrographs reveal localized agglomeration and interfacial voids caused by particle clustering and incomplete polymer encapsulation. Such features are commonly observed at high filler loadings and are known to weaken mechanical performance by introducing stress concentrators [35,36]. Such imperfections may act as stress concentrators and can reduce the local reinforcing efficiency at high filler loadings. However, in the present composites, the tensile strength still increased up to 25 wt% AC, indicating that mechanical interlocking between the rough, porous AC particles and the polymer matrix, together with network reinforcement effects, outweighed the adverse influence of localized agglomeration. At these higher AC contents, the formation of a denser and more continuous filler network also enhances electrical connectivity, which is beneficial for electromagnetic interference (EMI) shielding performance. Overall, the morphological results confirm that the recycled PE/PP matrix can effectively accommodate AC up to about 15 wt% with good dispersion and interfacial compatibility, while further increases in AC content promote network formation that influences both mechanical reinforcement and functional properties.

Density

The measured density of recycled PE/PP-AC composites at various filler loadings is shown in **Figure 3**. The density of the unfilled recycled PE/PP blend was 0.8987 g/ cm^3, and it increased progressively with the addition of AC. At 5 wt% AC, the density rose to 0.9134 g/cm^3, reaching 0.9627 g/ cm^3 at 25 wt%. This steady increase corresponds to the inherently higher density of AC compared with that of the recycled polymer matrix, consistent with the rule of mixtures. Comparable trends were observed in NR/Cu-AC composites [24] and PVDF-HFP/amethyst systems [37], where the addition of high-density fillers similarly increased composite density. The nearly linear trend confirms that AC particles were effectively incorporated into the recycled PE/PP matrix without the formation of significant voids

or porosity during melt blending and compression molding. This finding aligns with the SEM observations, where uniform dispersion and good interfacial adhesion were evident.

The higher density values also suggest more compact molecular packing and improved filler-matrix interaction. Similar trends have been reported in carbon-filled thermoplastics, where the presence of rigid carbon particles enhances the overall mass and dimensional stability of the composites. Therefore, the gradual density increase with AC loading verifies the successful integration of AC and the structural uniformity of the recycled PE/PP-AC composites.

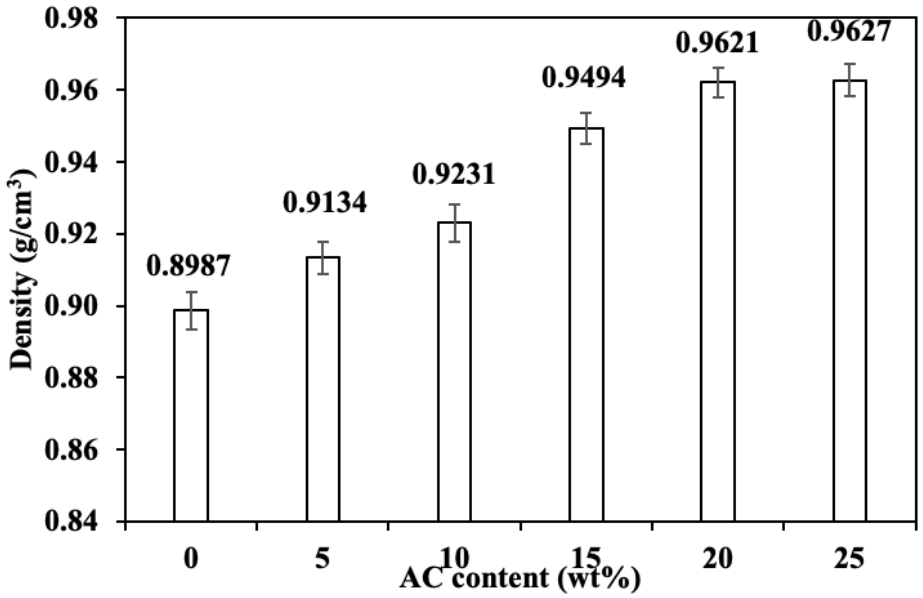

Figure 3 Density of recycled PE/PP-AC composites as a function of AC content.

Melt Flow Index (MFI)

The melt flow index (MFI) results of the recycled PE/PP-AC composites are shown in **Figure 4**. The unfilled recycled PE/PP blend exhibited an MFI of 58.29 g/10 min, reflecting the relatively high chain mobility of the recycled polyolefin matrix, which decreased steadily with increasing AC content, reaching 52.07 g/10 min at 5 wt% AC and 17.47 g/10 min at 25 wt%. This reduction in MFI reflects a progressive increase in melt viscosity as the AC loading increases [38]. The incorporation of rigid AC particles restricts polymer chain mobility and intensifies flow resistance during processing. This reduction in melt flow is primarily attributed to physical confinement effects, whereby the presence of rigid AC particles limits the free movement of PE/PP chains within the melt. Furthermore, the high surface area and porous texture of AC promote interfacial friction and physical entanglement between the filler surfaces and polymer chains, further hindering melt flow. Because no compatibilizers or surface treatments were applied to the AC, the interaction between AC and the PE/PP matrix is expected to be dominated by physical confinement and interfacial friction rather than specific chemical bonding at the filler-polymer interface. This mechanism is consistent with the behavior reported for activated-carbon-filled elastomeric systems, where increased filler rigidity and strong interfacial interactions reduce molecular mobility and increase viscosity [39].

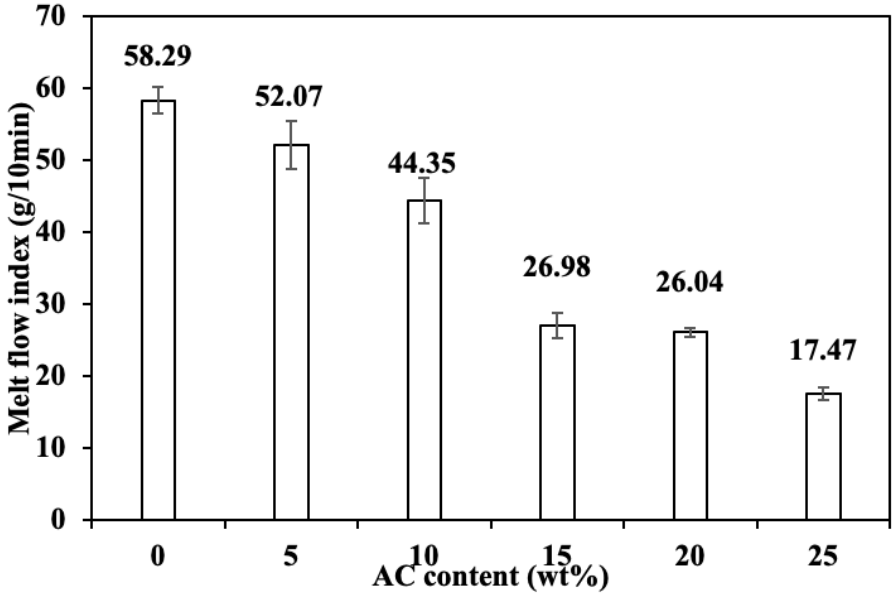

Figure 4 Melt flow index of recycled PE/PP-AC composites as a function of AC content.

The observed trend agrees with previous studies on carbon-based fillers in thermoplastics, where the incorporation of conductive and high-surface area fillers increase viscosity due to particle-matrix interaction and formation of microstructural networks [40,41]. From a structure-property perspective, the steady decline in MFI indicates reduced chain mobility arising mainly from physical confinement of the polymer chains. Such confinement-induced reductions in chain mobility have been widely associated with enhanced stiffness, improved dimensional stability, and the formation of conductive microstructural networks in filled polymer systems, as reported by Mishra *et al*. [42]. Accordingly, these effects are expected to contribute to the mechanical reinforcement and EMI shielding behavior discussed in the subsequent sections. The steady decline in MFI also suggests improved dimensional stability of the composites during molding, which is advantageous for producing recycled polymer products with consistent quality. Overall, the decreasing MFI with increasing AC content confirms restricted chain mobility and strong physical interactions between the recycled PE/PP matrix and activated carbon, in agreement with the SEM observations.

Mechanical properties

The effect of AC loading on the mechanical performance of the recycled PE/PP composites is presented in **Figure 5**. All key properties—tensile modulus, tensile strength, and elongation at break—showed a progressive increase with increasing AC content, indicating that the rigid carbon particles acted as effective reinforcing agents within the recycled polymer matrix. The tensile modulus increased from 1228 MPa for the unfilled blend to 1643 MPa at 25 wt% AC. This enhancement reflects the ability of stiff filler particles to restrict the mobility of polymer chains and improve stress transfer across the composite interface, a mechanism widely reported for polymer systems containing rigid particulate reinforcements [43,44]. The tensile strength followed a similar upward trend, rising from 7.7 MPa for the unfilled sample to 16.8 MPa at 25 wt% AC. This improvement can be attributed to strong filler-matrix interfacial adhesion and relatively uniform dispersion at moderate AC loadings, which promote efficient load transfer from the ductile polymer phase to the stiffer carbon particles. Comparable reinforcement behavior has been observed in biowaste-filled natural rubber composites, where well-dispersed rigid particles significantly enhance tensile strength through mechanical interlocking and interfacial bonding [45].

The elongation at break also increased markedly, from 7.7% for the unfilled composite to 16.8% at 25 wt% AC. This simultaneous improvement in both strength and ductility suggests that the rough and porous morphology of AC facilitates energy dissipation during deformation through mechanisms such as interfacial friction, crack deflection, and microstructural

toughening. Similar fracture-energy enhancement associated with rough filler surfaces has been documented in biowaste-filled elastomers and polyolefin blends, where complex filler–matrix interactions promote stable plastic deformation [44,45]. Overall, the mechanical results confirm that AC provides an effective balance of stiffness, strength, and toughness in the recycled PE/PP matrix. The combined reinforcing and energy-dissipating functions of the AC filler result in composites with improved structural reliability, making them suitable for functional applications where enhanced mechanical performance and sustainability are both required.

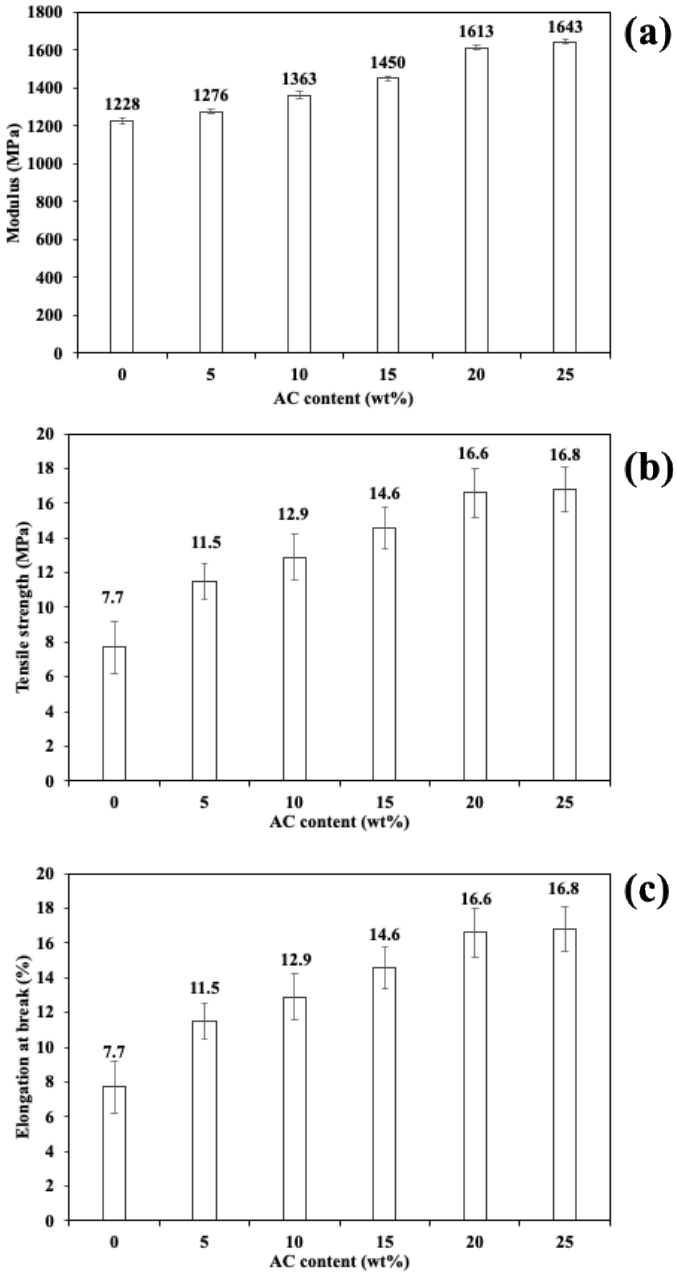

Figure 5 Tensile modulus (a), tensile strength (b), and elongation at break (c) of recycled PE/PP-AC composites at different AC loadings.

Thermal behavior

The differential scanning calorimetry (DSC) thermograms of the recycled PE/PP-AC composites during the first heating and cooling cycles are shown in **Figures 6(a)** - **6(b)**, with the corresponding thermal parameters summarized in **Table 2**. All samples

exhibited two distinct melting peaks: The lower-temperature peak (T_{m1} around 127 - 130 °C) corresponds to polyethylene (PE), while the higher-temperature peak (T_{m2} around160 - 165 °C) is associated with polypropylene (PP). The presence of both peaks confirms the coexistence of separate PE and PP crystalline domains within the recycled blend, a behavior widely reported for immiscible polyolefin blends [46]. With the incorporation of AC, both Tm_1 and T_{m2} shifted slightly upward up to 15 wt% AC. This behavior indicates that AC acts as a heterogeneous nucleating agent, promoting more ordered chain packing and facilitating crystal formation during reheating. Similar nucleation-driven shifts in melting temperature have been observed in polymer composites containing high-surface area fillers such as $FeCl_3 \cdot 6H_2O$ and graphene nanoplatelets [43]. The enhanced melting temperatures at moderate AC contents suggest improved thermal stability of the crystalline domains, which is beneficial for maintaining mechanical integrity under elevated service temperatures.

At higher AC loadings (20 - 25 wt%), a slight decrease in Tm_2 was noted, suggesting that excessive AC generates steric hindrance and disrupts polymer chain alignment, reducing crystalline perfection. Comparable reductions in melting temperature and crystallinity at elevated filler concentrations have been reported in carbon-based and nanoparticle-filled composites due to particle agglomeration and restricted chain mobility [44,45]. The crystallization temperature (T_c) during cooling exhibited a small upward shift from 121.22 °C for unfilled PE/PP to 122.24 °C at 20 wt% AC, confirming the nucleating role of AC in accelerating crystallization. The crystallization enthalpy (ΔH_c) increased substantially at moderate AC levels (5 - 10 wt%), reaching 574 and 564.55 J/g, respectively. This enhancement reflects improved nucleation efficiency, consistent with the crystallization behavior observed in polyolefin blends where heterogeneous nucleation accelerates crystal formation [46].

Table 2 Melting temperature (T_{m1}, T_{m2}), crystallization temperature (T_c), and crystallization enthalpy (ΔH_c) of recycled PE/PP-AC composites.

Sample	T_{m1}(°C)	T_{m2}(°C)	T_c (°C)	ΔH_c (J/g)
Recycled PE/PP (unfilled)	127.70	161.90	121.22	423.34
Recycled PE/PP + 5 wt% AC	128.13	162.76	121.51	574.00
Recycled PE/PP + 10 wt% AC	128.95	163.54	121.77	564.55
Recycled PE/PP + 15 wt% AC	129.43	164.35	121.93	499.53
Recycled PE/PP + 20 wt% AC	128.15	164.52	122.24	399.00
Recycled PE/PP + 25 wt% AC	126.64	159.84	121.77	364.39

The increase in ΔH_c further indicates enhanced crystallinity arising from efficient heterogeneous nucleation, consistent with reports showing that well-dispersed fillers facilitate lamellar growth and promote more ordered crystal structures [45]. Higher crystallinity at these filler contents is expected to contribute to increased stiffness and improved dimensional stability, which are beneficial for maintaining structural performance during prolonged service conditions. This structure-property relationship is well established for semi-crystalline polyolefin composites, where enhanced crystallinity leads to improved mechanical stability and resistance to deformation, as reported by Yang *et al*. [47]. Beyond 15 wt% AC, ΔH_c decreased progressively, which can be attributed to filler agglomeration that impedes lamellar growth and reduces the mobility required for complete crystallization, an effect similarly documented in nanoparticle-filled polymer systems [14,44]. Such reductions in crystallinity at excessive filler loadings may adversely affect long-term mechanical stability by introducing structural heterogeneities and localized stress concentrations. The DSC results confirm that moderate AC incorporation (≤15 wt%) enhances the crystallinity of the recycled PE/PP blend through heterogeneous nucleation and improved chain ordering. These crystallization effects

are expected to support improved mechanical stability and thermal reliability of the composites under service conditions, whereas excessive AC loading leads to agglomeration-driven disruption of crystalline order.

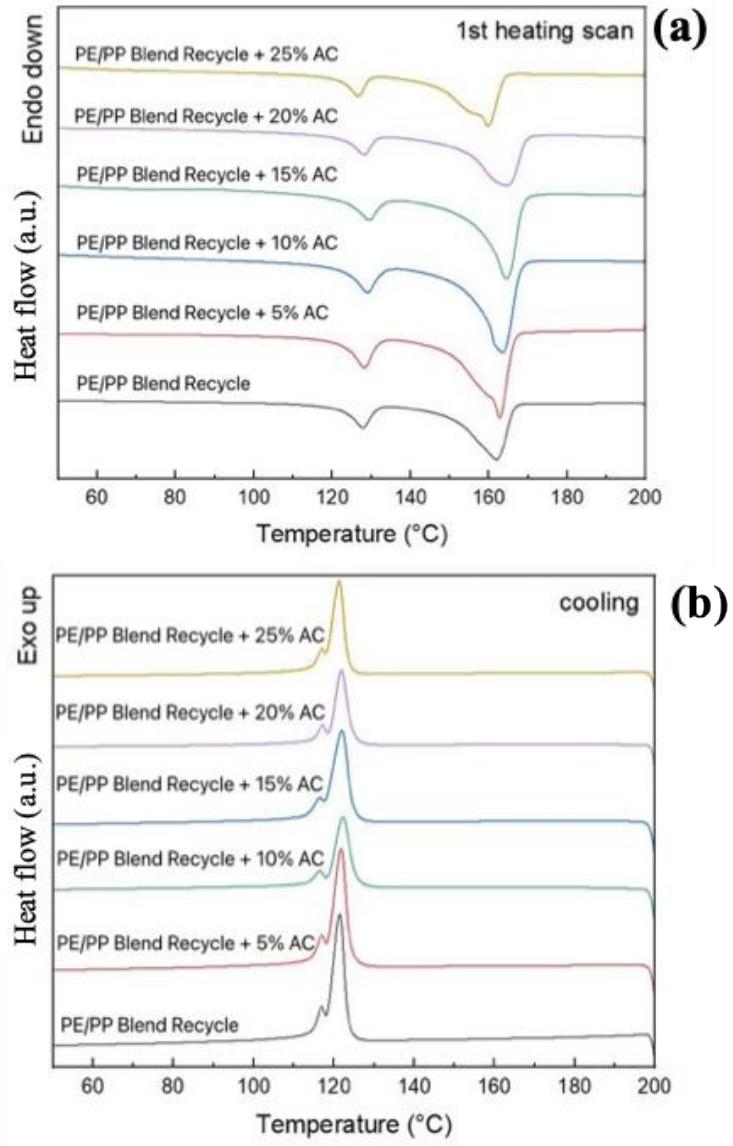

Figure 6 DSC thermograms of recycled PE/PP-AC composites: (a) First heating and (b) Cooling cycles.

Electromagnetic interference (EMI) shielding performance

The EMI-shielding performance of the recycled PE/PP-AC composites was evaluated over the 1 - 6 GHz frequency range, with representative spectra for the unfilled and 25 wt% AC samples shown in **Figures 7(a) - 7(b)**. The complete spectra for the intermediate AC loadings (5 - 20 wt%) are presented in the Supplementary Information (**Figures S1 - S4**), and the main attenuation minima are summarized in **Table 3**. The unfilled recycled PE/PP blend exhibited only modest shielding, with transmitted-signal minima of 6.82 dBμV at 2.22 GHz, –4.55 dBμV at 4.72 GHz, and –8.64 dBμV at 5.67 GHz. This weak shielding behavior is consistent with the inherently insulating nature of polyolefins, where electromagnetic waves are largely reflected at the material surface due to impedance mismatch, with minimal energy dissipation within the bulk matrix [6,48]. In this case, EMI attenuation is dominated by surface reflection, and absorption mechanisms are negligible.

With the incorporation of AC, a clear reduction in transmitted-signal intensity (stronger EMI attenuation) was observed. At low AC loading (5 wt%), attenuation

minima of 14.64 dBμV at 2.46 GHz and –2.50 dBμV at 3.88 GHz were recorded. This behavior suggests the onset of interfacial polarization and localized micro-conductive regions, arising from the introduction of electrically active carbon particles into the insulating PE/PP matrix. Increasing the filler content to 10 wt% AC further enhanced attenuation, with minima of 12.14 dBμV at 2.20 GHz and 7.14 dBμV at 3.87 GHz, reflecting increased dielectric loss and charge-hopping processes at polymer-filler interfaces [49]. More pronounced attenuation occurred at higher filler loadings (15 - 25wt. %). For 15 wt% AC, transmitted-signal minima of 16.30 dBμV at 2.40 GHz and 2.30 dBμV at 4.15 GHz were recorded, while 20 wt% AC produced three distinct minima: 5.71 dBμV at 2.17 GHz, 3.57 dBμV at 3.88 GHz, and 10.71 dBμV at 4.80 GHz. These features indicate the development of semi-continuous conductive pathways, which facilitate charge transport, dielectric relaxation, and multiple internal reflections within the composite [50].

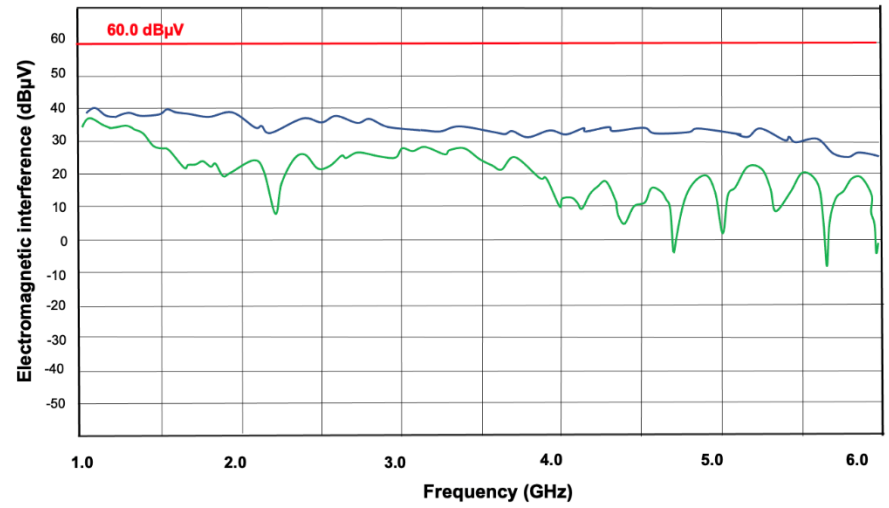

(a)

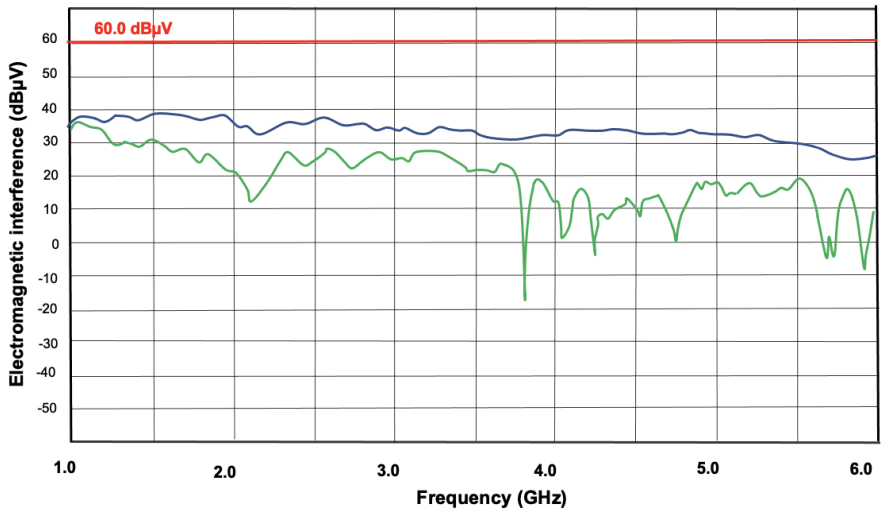

(b)

Figure 7 Representative EMI-shielding spectra of recycled PE/PP-AC composites measured over 1 - 6 GHz: (a) Unfilled recycled PE/PP and (b) Recycled PE/PP with 25 wt% activated carbon (AC). The red, blue, and green curves correspond to the reference input signal, baseline response, and transmitted signal, respectively. A lower transmitted-signal intensity (green curve) indicates stronger EMI-shielding effectiveness.

Table 3 Characteristic attenuation minima (frequency and signal intensity) of recycled PE/PP-AC composites in the 1 - 6 GHz range.

AC (wt%)	f_1 (GHz)	Min_1 (dBμV)	f_2 (GHz)	Min_2 (dBμV)	f_3 (GHz)	Min_3 (dBμV)
Unfilled	2.22	6.82	4.72	–4.55	5.67	–8.64
5 wt%	2.46	14.64	3.88	–2.50	-	-
10 wt%	2.20	12.14	3.87	7.14	-	-
15 wt%	2.40	16.30	4.15	2.30	-	-
20 wt%	2.17	5.71	3.88	3.57	4.80	10.71
25 wt%	2.15	11.36	3.82	–18.64	5.93	–7.14

The strongest EMI-shielding performance was achieved at 25 wt% AC, where the transmitted-signal minima reached 11.36 dBμV at 2.15 GHz, –18.64 dBμV at 3.82 GHz, and –7.14 dBμV at 5.93 GHz. These pronounced attenuation minima indicate the development of a semi-continuous conductive network, which is a key characteristic of absorption-dominated EMI shielding behavior in carbon-based polymer composites, as previously reported by Durmaz *et al*. [51]. At this filler concentration, the high specific surface area and partially graphitic microstructure of AC introduce numerous polarization centers and conductive pathways, promoting interfacial polarization, dipole relaxation, and charge-hopping processes. As a result, incident electromagnetic waves entering the composite are efficiently dissipated through a combination of dielectric and conductive losses rather than being simply reflected at the surface [50,52]. These attenuation trends correlate well with the SEM observations, which showed increasingly dense AC networks and improved contact between the filler and the polymer matrix as the filler loading increases. As a result, the dominant EMI shielding mechanism in the recycled PE/PP-AC composites develops from mainly surface reflection at low activated carbon contents to absorption-dominated attenuation involving multiple internal reflections within the bulk material at higher loadings. Such absorption-based shielding is particularly desirable, as it reduces secondary electromagnetic radiation and improves overall shielding reliability [50]. Generally, the results demonstrate that incorporating coconut-shell-derived AC into recycled PE/PP yields lightweight, low-cost, and environmentally friendly composites with promising EMI-shielding capability for electronic housings, signal-protection components, and low-frequency interference-control applications.

Structure-property correlation

The results presented in this study show a clear structure-property relationship that governs the multifunctional performance of the recycled PE/PP-AC composites. The incorporation of AC substantially reformed the microstructural organization of the PE/PP blend, which in turn dictated its mechanical, thermal, and electromagnetic responses. AC particles were uniformly dispersed in the recycled PE/PP matrix up to approximately 15 wt%, producing strong interfacial adhesion and enabling efficient stress transfer. This well-dispersed microstructure corresponds directly with the mechanical reinforcement, where the rough, porous surface of AC promoted mechanical interlocking and facilitated effective load distribution, resulting in higher tensile modulus and strength. At higher filler contents (≥20 wt%), however, localized agglomeration and interfacial voids were observed, generating stress concentration sites that partially diminished the reinforcing efficiency of the AC particles. The thermal behavior of the composites further supports this correlation. Moderate AC additions (≤15 wt%) increased the crystallization enthalpy (ΔHc) and slightly elevated both melting and crystallization temperatures, confirming the role of AC as a heterogeneous nucleating agent. The improvement in crystalline ordering and constrained chain mobility is consistent with the enhanced stiffness and dimensional stability observed mechanically. In contrast, excessive AC loadings disrupted crystalline development and reduced ΔH_c, mirroring the decrease in mechanical performance caused by particle clustering and reduced polymer

mobility. These microstructural and thermal developments directly influenced the electromagnetic shielding performance. At higher AC concentrations, the formation of a semi-continuous conductive network enabled interfacial polarization, multiple internal reflections, and ohmic loss, facilitating the conversion of electromagnetic energy into heat. The same filler network responsible for improved rigidity and nucleation efficiency also provided continuous pathways for charge transport and dielectric loss, demonstrating a strong interdependence between microstructure and functional performance. This behavior aligns well with recent design principles for sustainable carbon-based functional composites, where porosity, graphitic domains, and filler network formation are identified as key parameters governing both mechanical reinforcement and absorption-dominated EMI shielding, as highlighted by Zhang *et al*. [53]. More broadly, the integration of bio-derived carbon fillers into polymer matrices for multifunctional performance aligns with established strategies for sustainable functional materials, where renewable carbon sources enable conductive networks and mechanically robust architectures for electronic and structural applications, as discussed by Zhu *et al*. [54].

Generally, the performance of the recycled PE/PP-AC composites arises from a balance between filler dispersion, interfacial adhesion, and conductive network continuity. The most favorable combination of mechanical reinforcement, thermal stability, and EMI-shielding effectiveness was achieved at 10 - 15 wt% AC, where the composite maintained good dispersion without severe agglomeration. These results highlight the potential of combining recycled polymers with bio-derived activated carbon to produce sustainable, multifunctional composites with tunable mechanical and electromagnetic properties.

Conclusions

Recycled PE/PP composites filled with activated carbon (AC) were successfully developed, exhibiting simultaneous improvements in mechanical strength, thermal stability, and electromagnetic shielding efficiency. The density increased from 0.8987 to 0.9627 g/cm^3, while the melt flow index decreased from 58.29 to 17.47 g/10 min, indicating strong filler-matrix interaction. The tensile modulus and strength rose to 1643 and 16.8 MPa, respectively, accompanied by improved toughness. DSC results revealed dual melting peaks at around 128 °C and around 163 °C with a higher crystallization temperature (122.24 °C) and enthalpy (ΔH_c = 574 J/g at 5 wt% AC), which confirm the role of AC as a nucleating agent. EMI-shielding performance also improved with increasing AC content. The strongest attenuation occurred in the 25 wt% AC composites, which exhibited a minimum transmitted-signal intensity of –18.64 dBμV at 3.82 GHz, attributed to the development of semi-continuous conductive networks and enhanced dielectric loss mechanisms. These findings demonstrate that the combination of recycled PE/PP and bio-based AC provides an eco-friendly and cost-effective route to create lightweight composites with enhanced mechanical and functional performance of recycled PE/PP composites for sustainable EMI-shielding applications.

Acknowledgements

This work was supported by the Department of Materials and Metallurgical Engineering and Department of Electronics and Telecommunication Engineering, Faculty of Engineering, Rajamangala University of Technology Thanyaburi, Pathum Thani 12110, Thailand.

Declaration of Generative AI in Scientific Writing

The authors acknowledge the use of generative tools (e.g., Quill Bot and Grammarly) solely for language editing and grammar refinement during manuscript preparation. No content generation or data interpretation was performed by AI. The authors take full responsibility for all findings, interpretations, and conclusions presented in this work.

CRediT Author Statement

Waroonsiri Jakrabutr: Conceptualization, Methodology, Formal analysis, Data curation, Investigation, Resources, Writing – original draft. **Kullawadee Sungsanit:** Conceptualization, Methodology, Validation, Formal analysis, Data curation, Writing – original draft. **Suchalinee Mathurosemontri:** Methodology, Validation, Formal analysis, Data curation, Writing – original draft. **Nichanan Phansroy:** Methodology, Validation, Formal analysis, Data curation, Writing – original draft.

Phongsuk Ampha: Software, Investigation. **Nathapong Sukhawipat:** Conceptualization, Methodology, Validation, Writing – review & editing. **Jureeporn Yuennan:** Methodology, Validation, Formal analysis, Data curation, Writing – original draft. **Wichain Chailad:** Conceptualization, Methodology, Validation, Investigation, Formal analysis, Data curation, Writing – original draft, Writing – review & editing, Supervision, Project administration.

References

[1] AA Isari, A Ghaffarkhah, SA Hashemi, S Wuttke and M Arjmand. Structural design for EMI shielding: From underlying mechanisms to common pitfalls. *Advanced Materials* 2024; **36(24)**, 2310683.

[2] JP Filipovic, M Milenkovic, D Kepic, S Dorontic, M Yasir, B Nardin and S Jovanovic. Electromagnetic interference in the Modern Era: Concerns, trends, and nanomaterial-based solutions. *Nanomaterials* 2025; **15(20)**, 1558.

[3] MA Morales, TC Henry and LG Salamanca-Riba. Model of electromagnetic interference shielding effectiveness for a multifunctional composite containing carbon-fiber-reinforced polymer and copper mesh layers. *Carbon* 2023; **212**, 118179.

[4] D Wanasinghe and F Aslani. A review on recent advancement of electromagnetic interference shielding novel metallic materials and processes. *Composites Part B: Engineering* 2019; **176**, 107207.

[5] D Jiang, V Murugadoss, Y Wang, J Lin, T Ding, Z Wang, Q Shao, C Wang, H Liu, N Lu, R Wei, A Subramania and Z Guo. Electromagnetic interference shielding polymers and nanocomposites - a review. *Polymer Reviews* 2019; **59(2)**, 280-337.

[6] F Safdar, M Ashraf, A Javid and K Iqbal. Polymeric textile-based electromagnetic interference shielding materials, their synthesis, mechanism and applications – a review. *Journal of Industrial Textiles* 2022; **51(5)**, 7293-7358.

[7] H Zhang and S Lin. Research progress with membrane shielding materials for electromagnetic/radiation contamination. *Membranes* 2023; **13(3)**, 315.

[8] V MG, M Vatnalmath and V Auradi. A review on conductive polymer composites focusing on advancements in electrical conductivity, and electromagnetic shielding capabilities. *Polymer Composites* 2025; **46(18)**, 16507-16537.

[9] F Xie, Q Liu, X Dai, H Wei and Z Lu. Highly durable hollow sandwich MXene/h-AgNWs/ANF composite films for exceptional electromagnetic interference shielding performance. *Composites Science and Technology* 2024; **256**, 110766.

[10] GM Mamatha, P Dixit, RH Krishna and SG Kumar. Polymer based composites for electromagnetic interference (EMI) shielding: The role of magnetic fillers in effective attenuation of microwaves, a review. *Hybrid Advances* 2024; **6**, 100200.

[11] Y Wang, W Zhao, L Tan, Y Li, L Qin and S Li. Review of polymer-based composites for electromagnetic shielding application. *Molecules* 2023; **28(15)**, 5628.

[12] Y Zhang, M Qiu, Y Yu, B Wen and L Cheng. A novel polyaniline-coated bagasse fiber composite with core–shell heterostructure provides effective electromagnetic shielding performance. *ACS Applied Materials & Interfaces* 2017; **9(1)**, 809-818.

[13] H Zhao, L Hou, S Bi and Y Lu. Enhanced X-band electromagnetic-interference shielding performance of layer-structured fabric-supported Polyaniline/Cobalt–Nickel coatings. *ACS Applied Materials & Interface* 2017; **9(38)**, 33059-33070.

[14] W Chailad, P Nanthananon, W Jakarbutr, N Phansroy and S Mathurosemontri. Impact of graphene nanoplatelet size and hybridisation on the properties of natural rubber nanocomposites. *Journal of Polymer Research* 2024; **31**, 223.

[15] V Yadav, D Pal and AK Poonia. Nanofillers as a potential key for shaping the future of the industries. *Hybrid Advances* 2024; **7**, 100340.

[16] D Li, C Dong, AP Zhang, HL Lin, BY Peng, KY Ni, KC Yang, J Bian and DQ Chen. Polymer-based composites for electromagnetic interference shielding: Principles, fabrication, and applications. *Composites Part A: Applied Science and Manufacturing* 2025; **194**, 108927.

[17] Y Zhang and J Gu. A perspective for developing polymer-based electromagnetic interference shielding composites. *Nano-Micro Letters* 2022;

14, 89.

[18] R Seidel, K Katzer, J Bieck, M Langer, J Hesselbach and M Heilig. Influence of carbon-based fillers on the electromagnetic shielding properties of a silicone-potting compound. *Materials* 2024; **17(2)**, 280.

[19] B Ucpinar and A Aytac. Promising electromagnetic interference shielding materials: Hybrid fillers reinforced bio-based composites. *Journal of Applied Polymer Science* 2025; **142(12)**, 56618.

[20] Shivani, J Vishwakarma, DK Rajak, R Kumar, C Dhand, A Mishra and N Dwivedi. Sustainable approaches based on waste materials for developing electromagnetic radiation shielding systems. *Next Materials* 2025; **9**, 101285.

[21] EC Gokce, MD Calisir, S Selcuk, M Gungor and ME Acma. Electromagnetic interference shielding using biomass-derived carbon materials. *Materials Chemistry and Physics* 2024; **317**, 129165.

[22] M Mehmandoust, G Li and N Erk. Biomass-derived carbon materials as an emerging platform for advanced electrochemical sensors: Recent advances and future perspectives. *Industrial & Engineering Chemistry Research* 2022; **62(11)**, 4628-4635.

[23] YJ Yim and BJ Kim. Preparation and characterization of activated carbon/polymer composites: A review. *Polymers* 2023; **15(16)**, 3472.

[24] W Chailad, W Ariyawiriyanan, S Pavasupree, N Sosa, Y Wongnongwa, J Yuennan, E Martwong, SIN Ayutthaya, L Yang and N Sukhawipat. Elastomeric dielectric materials from natural rubber/copper-modified coconut-shell-derived activated carbon composite: Combined experimental and density functional theory study. *Industrial Crops and Products* 2025; **234**, 121511.

[25] JY Yusuf, H Soleimani, N Yahya, YK Sanusi, G Kozlowski, A Öchsner, LL Adebayo, FA Wahaab, S Sikiru and BB Balogun. Electromagnetic wave absorption of coconut fiber-derived porous activated carbon. *Boletín de la Sociedad Española de Cerámica y Vidrio* 2022; **61(5)**, 417-427.

[26] SUD Khan, M Arora, MA Wahab and P Saini. Permittivity and electromagnetic interference shielding investigations of activated charcoal loaded acrylic coating compositions. *Journal of Polymers* 2014; **2014**, 193058.

[27] L Umdagas, R Orozco, I Kings, W Thom and B Al-Duri. Advances in chemical recycling of polyolefins by hydrothermal liquefaction in supercritical water: A comprehensive review. *The Journal of Supercritical Fluids* 2026; **227**, 106761.

[28] L Carvalho, G Mattos, N Sitton, J Barros, D Miranda, R Luciano and JC Pinto. A survey on the chemical recycling of polyolefins into monomers. *Processes* 2025; **13(7)**, 2114.

[29] C Aumnate, N Rudolph and M Sarmadi. Recycling of polypropylene/polyethylene blends: Effect of chain structure on the crystallization behaviors. *Polymers* 2019; **11(9)**, 1456.

[30] B Gayretli, R Shanthar, TT Öpöz and C Abeykoon. Mechanical properties of LDPE and PS polymer matrix composites reinforced with GNP and CF — A critical review. *International Journal of Lightweight Materials and Manufacture* 2024; **7(4)**, 572-596.

[31] S Saikrishnan, D Jubinville, C Tzoganakis and TH Mekonnen. Thermo-mechanical degradation of polypropylene (PP) and low-density polyethylene (LDPE) blends exposed to simulated recycling. *Polymer Degradation and Stability* 2020; **182**, 109390.

[32] C Rosales, N Aranburu, I Otaegi, V Pettarin, C Bernal, AJ Müller and G Guerrica-Echevarría. Improving the mechanical performance of LDPE/PP blends through microfibrillation. *ACS Applied Polymer Materials* 2022; **4(5)**, 3369-3379.

[33] J Kruželák, A Kvasničáková, K Hložeková and I Hudec. Progress in polymers and polymer composites used as efficient materials for EMI shielding. *Nanoscale Advances* 2021; **3(1)**, 123-172.

[34] MMA Nassar, KI Alzebdeh, MMM Alsafy and M Jawaid. Optimization and predictive modelling of chemically crosslinked recycled PE/PP blends for enhanced mechanical properties. *Results in Engineering* 2025; **28**, 108360.

[35] W Chailad, K Tongsom, K Chaochanchaikul and C Sakulkhaemaruethai. Enhancing air retention in

natural rubber: A path to improved performance. *Polymer Bulletin* 2025; **82**, 3841-3866.

[36] C Sakulkhaemaruethai, S Sakulkhaemaruethai, A Pholsuwan and W Chailad. Flame-retardant natural rubber composites: the synergistic role of zeolite and aluminium trihydrate. *Polymer Bulletin* 2025; **82**, 7427-7446.

[37] W Chailad, J Yuennan, N Tohluebaji, P Nuchnong, Y Tran, E Martwong, L Yang and N Sukhawipat. Silane-modified waste amethyst as a functional filler in PVDF-HFP composites for flexible dielectric and energy applications. *Journal of Materials Science* 2025; **60**, 25297-25321.

[38] NAA Rahim, ZM Ariff, A Ariffin and SS Jikan. Study on effect of filler loading on the flow and swelling behaviors of polypropylene-kaolin composites using single-screw extruder. *Journal of Applied Polymer Science* 2010; **119(1)**, 73-83.

[39] EP Wulandari, P Marlina, Nasruddin, Lanjar, H Yohanes, WE Widodo, SJ Munarso, Astuti, EB Susetyo, Y Bakhtiar, H Guo and WB Setianto. Application of sawdust-derived activated carbon as a bio-based filler in vulcanized rubber bushings. *Polymers* 2025; **17(22)**, 2996.

[40] A Kasgoz, D Akın, Aİ Ayten and A Durmus. Effect of different types of carbon fillers on mechanical and rheological properties of cyclic olefin copolymer (COC) composites. *Composites Part B: Engineering* 2014; **66**, 126-135.

[41] VM Nazarychev, GV Vaganov, SV Larin, AL Didenko, VY Elokhovskiy, VM Svetlichnyi, VE Yudin and SV Lyulin. Rheological and mechanical properties of thermoplastic crystallizable polyimide-based nanocomposites filled with carbon nanotubes: Computer simulations and experiments. *Polymers* 2022; **14(15)**, 3154.

[42] DC Kong, MH Yang, XS Zhang, ZC Du, Q Fu, XQ Gao and JW Gong. Control of polymer properties by entanglement: A review. *Macromolecular Materials and Engineering* 2021; **306(12)**, 2100536.

[43] J Yuennan, N Muensit, N Tohluebaji, W Chailad, L Yang, N Sukhawipat, GA Ashraf and P Channuie. Tailoring dielectric properties and crystallinity in poly(vinylidene fluoride-co-hexafluoropropylene) nanocomposites via iron (III) chloride hexahydrate incorporation. *Scientific Reports* 2025; **15**, 17810.

[44] H Jones, J McClements, D Ray, M Kalloudis and V Koutsos. High-density polyethylene–polypropylene blends: Examining the relationship between nano/microscale phase separation and thermomechanical properties. *Polymers* 2025; **17(2)**, 166.

[45] W Jakarbutr, K Sungsanit, S Mathurosemontri, N Phansroy, C Sakulkhaemaruethai, W Ariyawiriyanan, N Sukhawipat and W Chailad. Structure–property relationships in biowaste-filled natural rubber: Effects of particle size and ageing on mechanical and thermal performance. *Polymer Bulletin* 2025; **82**, 10197-10234.

[46] DE Huang, AP Kotula, CR Snyder and KB Migler. Crystallization kinetics in an immiscible polyolefin blend. *Macromolecules* 2022; **55(24)**, 10921-10932.

[47] V Dananjaya, M Yang, Y Zheng and C Abeykoon. Effect of filler characteristics and processing route on bamboo powder-reinforced PLA composites. *Journal of Cleaner Production* 2025; **537**, 147193.

[48] IS Sani, NR Demarquette and E David. Enhancing the dielectric properties of recycled polyolefin streams through blending. *Sustainability* 2025; **17(9)**, 4123.

[49] SS Hota, D Panda, R Panda, S Mishra, S Choudhury, L Biswal, RNP Choudhary and A Satapathy. Dielectric characteristics and energy storage capabilities of PVDF-based composite incorporating 2D GnP nanofiller. *Results in Engineering* 2025; **26**, 105593.

[50] C Wang, V Murugadoss, J Kong, Z He, X Mai, Q Shao, Y Chen, L Guo, C Liu, S Angaiah and Z Guo. Overview of carbon nanostructures and nanocomposites for electromagnetic wave shielding. *Carbon* 2018; **140**, 696-733.

[51] BU Durmaz, AO Salman and A Aytac. Electromagnetic interference shielding performances of carbon-fiber-reinforced PA11/PLA composites in the x-band frequency range. *ACS Omega* 2023; **8(25)**, 22762-22773.

[52] M Li, Q Xu, W Jiang, A Farooq, Y Qi and L Liu. Preparation and investigation of Fe3O4@rGO/CNF foams for electromagnetic

interference shielding. *Fibers and Polymers* 2023; **24**, 771-778.

[53] K Zhang, Z Huang, M Yang, M Liu, Y Zhou, J Zhan and Y Zhou. Recent progress in melt pyrolysis: Fabrication and applications of high-value carbon materials from abundant sources. *SusMat* 2023; **3(5)**, 558-580.

[54] H Zhu, W Luo, PN Ciesielski, Z Fang, JY Zhu, G Henriksson, ME Himmel and L Hu. Wood-derived materials for green electronics, biological devices, and energy applications. *Chemical Reviews* 2016; **116(16)**, 9305-9374.

Supplementary Information

Electromagnetic Shielding Spectra of Recycled PE/PP-AC Composites Additional EMI-shielding spectra for the recycled PE/PP–AC composites at intermediate AC loadings are provided to complement the representative data shown in **Figure 7**. The spectra were recorded in the frequency range of 1 - 6 GHz under identical measurement conditions. Each spectrum displays three traces: the red line, representing the reference input level (60 dBµV); the blue line, showing the baseline response; and the green line, corresponding to the transmitted signal intensity after interaction with the sample. The decrease in green-line intensity relative to the reference indicates the electromagnetic attenuation (shielding) achieved by the composite.

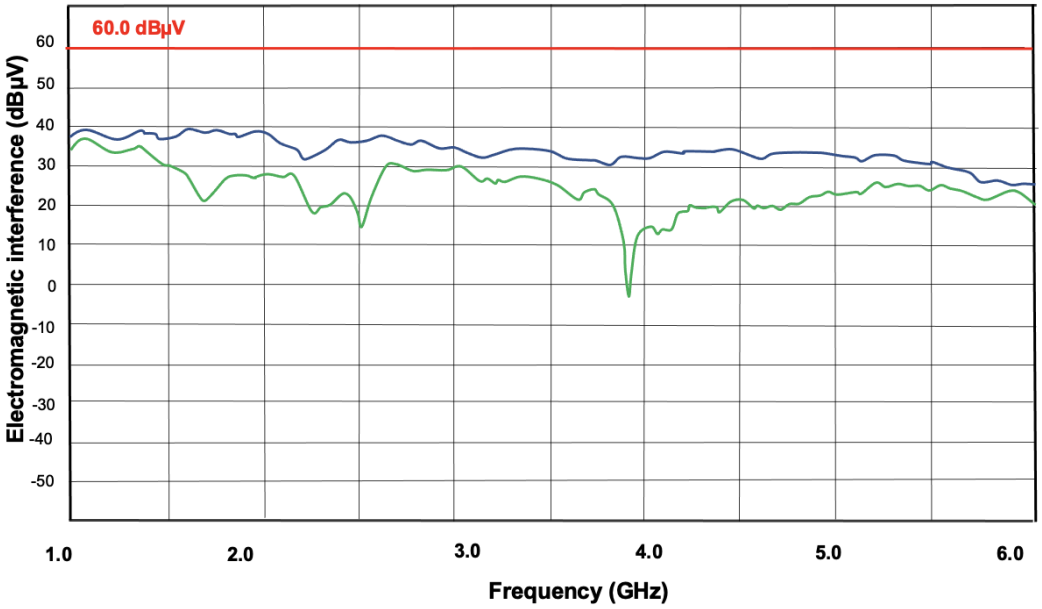

Figures S1 EMI-shielding spectrum of recycled PE/PP +5 wt% AC measured over 1 - 6 GHz.

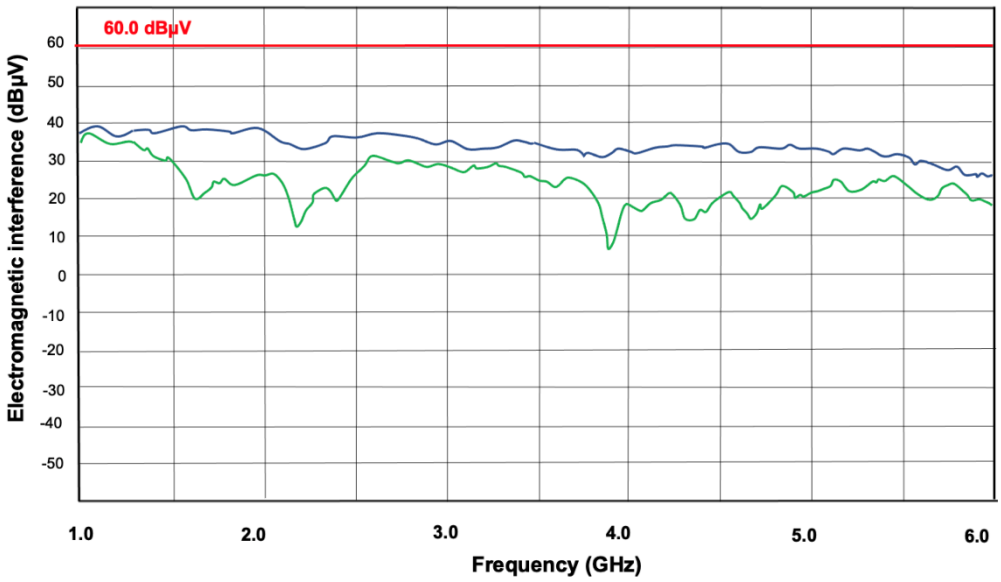

Figures S2 EMI-shielding spectrum of recycled PE/PP +10 wt% AC measured over 1 - 6 GHz.

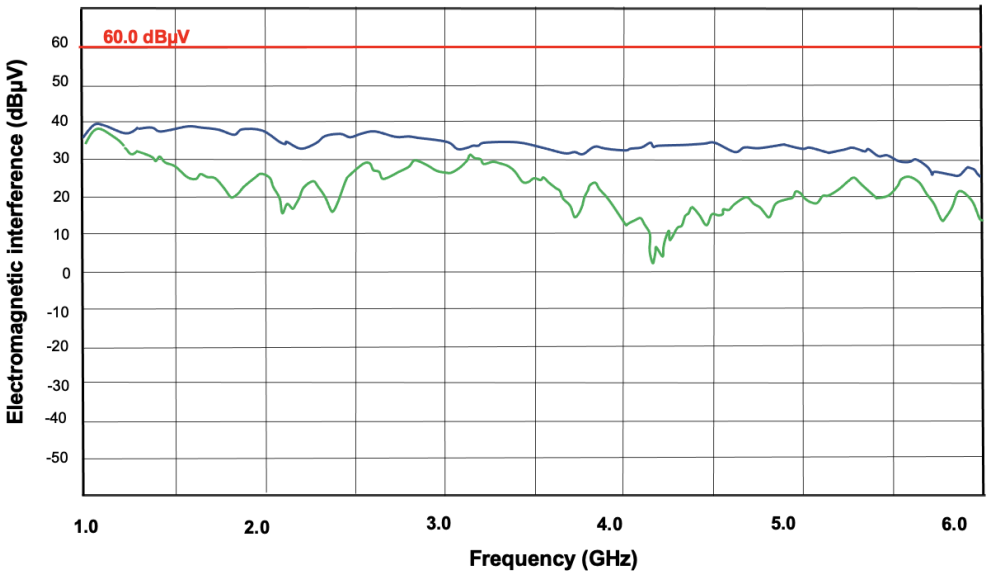

Figures S3 EMI-shielding spectrum of recycled PE/PP +15 wt% AC measured over 1 - 6 GHz.

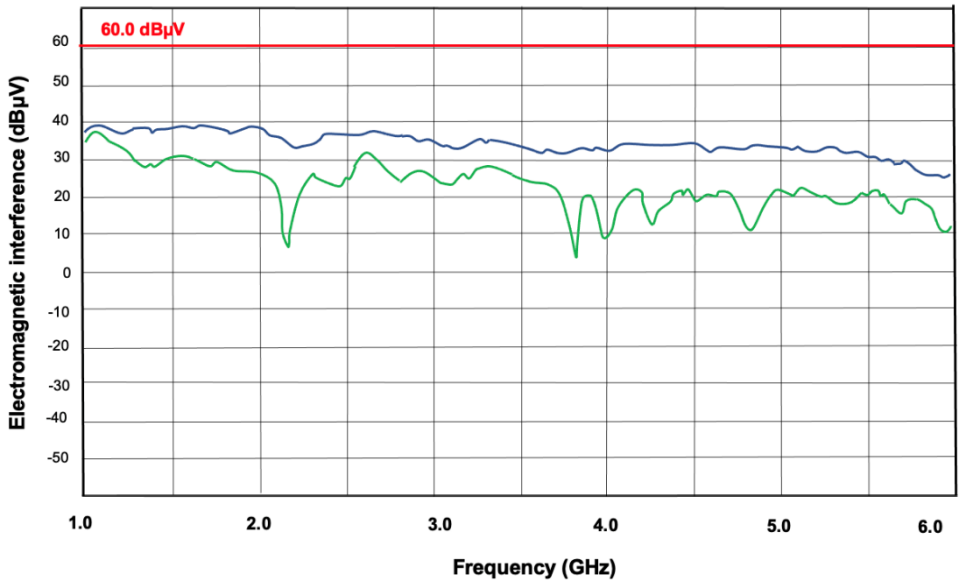

Figures S4 EMI-shielding spectrum of recycled PE/PP +20 wt% AC measured over 1 - 6 GHz.